Evaluation of the effect of different policies in the containment of epidemic spreads for the COVID-19 case [*]

Paolo Di Giamberardino and Daniela Iacoviello
Dept. of Computer, Control and Management Engineering
Sapienza University of Rome, Rome, Italy
paolo.digiamberardino@uniroma1.it
daniela.iacoviello@uniroma1.it

Abstract

The paper addresses the problem of analysing the effect of each different control action on the evolution of an epidemic spread for which no vaccine is available. It is specifically referred to the COVID-19 spread. A new mathematical model for virus propagation is described, designed to include all the possible actions to prevent the spread and to help in the healing of infected people. The analysis of the effect on the population for each different control action is performed showing where and how much they have effects in the spread dynamics.
Keywords: Epidemic model, COVID-19, spread reduction, effect forecast

1 Introduction

As for all dynamical systems, when dealing with epidemic spreads a mathematical model is at basis of realistic interpretation of the behaviours and of reliable forecast of the evolutions.

From the earliest contribution of [1], where the most simple but also the most used model, known as SIR (Susceptible, Infected and Recovered individuals), several richer and more specific models have been proposed in literature. A first step is [2], where a SIRC model is used to describe the influenza disease, to face the case of partial or temporarily limited immunity.

More recently, more complex models have been introduced, developed for specific classes of infections, to better describe their propagation and to particularize the specific control actions against their spread.

Then, for the HIV/AIDS disease, case in which no effective vaccine is known yet, the models have to classify the population into a higher number of classes

---

and, due to the severity of the disease, the interventions must be reconsidered with respect to a SIR or a SIRS [3–8].

Another relevant example is the measles disease [9–12]; in this case the vaccination is available but the relatively high number of immuno–depressed individuals needs additional controls and then a more specific mathematical models to include them [13].

At present, the worldwide ongoing COVID-19 due to the SARS-CoV-2 virus spread [14–17] presents the necessity to deal with different models. The definition of a mathematical model to describe the phenomenon [15], to estimate its diffusivity [18, 19] and to give a realistic forecasts to prepare the most suitable countermeasures [20] have represented the first contributions, but mainly referring or readapting known epidemic models. In [15], a quite rich model is proposed, composed by 8 different classes: in addition to the usual susceptible (S), exposed (E), infectious with symptoms (I) and recovered (R) compartments, there are also the groups of pre-symptomatic infectious (A), the hospitalized (H), the quarantined susceptible (Sq), the isolated exposed (Eq) and the isolated infected (Iq) compartments and the model parameters are on the basis of the the available data. The pandemic characteristics of the disease motivates also analysis as in [17], where geographical movements are considered.

Regarding the support for forecasting ability of a mathematical model, in [20] a short time forecast is provided, based on the uncertain data available and making reference to models developed for similar cases [21–24].

Due to the unavailability of a vaccine, like for the AIDS, in the COVID-19 case a mathematical model which has to be used for control design [10, 25–29] must include all possible lines of interventions to better distribute the efforts and then, hopefully, increase the effects.

To this aim, in this paper, a mathematical model for SARS-CoV-2 diffusion among the population, different from the ones previously presented, is introduced; all the known preventive and active actions that can be put in place, at an organizational and decisional level as well as from a medical point of view, to contain the virus spread and its negative consequences are considered.

This particular attention devoted to the control possibility brings, in this first analysis, to a characterization of the effects of each control on the system behaviour, for each class considered, in view of the design of effective and sustainable controls.

In Section 2 the model is introduced and illustrated, with a particular attention to the choices for the numerical values of the parameters. Section 3 contains the illustration and the description, through numerical simulations performed on the basis of the proposed model, of the effects of each single different control actions.

2   The mathematical model

The mathematical model here adopted is an enrichment of a classical SEIR model which is usually adopted to describe the dynamics of epidemic spreads

in presence of an virus incubation phase (E) during which the individuals are not yet infectious [30].

Making reference to the recent work [17] on the COVID-19, in this contribution two new classes are added and the possible ways of intervention are modelled in order to make available some numerical evaluations about the possible epidemic diffusion depending on the different action strategies.

In Subsection 2.1 the model is described; equilibrium conditions and stability properties are analysed in Subsection 2.2 while the analysis and the discussion of the effects of the controls on the dynamics is the topic of Section 3.

2.1 The mathematical model adopted

The mathematical model used is

$$
\begin{aligned}
\dot{S}(t) &= B - \beta(1 - u_2(t))S(t)I_C(t) + bnQ(t) + cnu_5(t)Q(t) \\
&\quad - au_1(t)S(t) - d_S S(t) && (1) \\
\dot{E}(t) &= \beta(1 - u_2(t))S(t)I_C(t) - au_1(t)E(t) - kE(t) - d_E E(t) && (2) \\
\dot{I}_C(t) &= kE(t) - au_1(t)I_C(t) - h_1 I_C(t) - h_2 I_C(t) - d_{I_C} I_C(t) && (3) \\
\dot{I}_Q(t) &= h_1 I_C(t) + h_1(1 - n)Q + c(1 - n)u_5(t)Q(t) \\
&\quad - (\gamma + \eta u_3(t)) I_Q(t) - d_{I_Q}(1 - u_4(t))I_Q(t) && (4) \\
\dot{Q}(t) &= au_1(t)\left(S(t) + E(t) + I_C(t)\right) - bnQ(t) - h_1(1 - n)Q \\
&\quad - cu_5(t)Q(t) - d_Q Q(t) && (5) \\
\dot{R}(t) &= h_2 I_C(t) + (\gamma + \eta u_3(t)) I_Q(t) - d_R R(t) && (6)
\end{aligned}
$$

where S are the susceptible people; E are the exposed individuals, infected but not infective; I_C are the infected patients without symptoms, asymptomatic until the healing or until symptoms arise: they are infective and then responsible of the disease spread; I_Q are the diagnosed infected patients, isolated and then not contagious: patients in this class are the ones that can receive medical treatment both for the infection and for secondary diseases or complications; Q are the suspected infected individuals which are temporarily isolated and tested for positivity of the SARS-CoV-2, or simply quarantined for safeness reasons; R are the recovered individuals, supposed to be no more infected.

As far as the model parameters is concerned, their meaning is as follows. All the d_* terms denote the death rates in each class. The term B denotes the constant inflow rate of new individuals. Coefficient β is the contagion rate. Parameters k, h_1, h_2 and γ denote the natural transition rates between classes: k is referred to the evolution of the illness, defied according to the rate of symptoms outbreak; h_1 describes the fraction of I_C that, after the symptoms, moves to the class of individuals I_Q, isolated or under therapies, while h_2 is the fraction of I_C that, in absence of symptoms, or underestimating the gravity, continues to infect susceptible individuals; both h_1 and h_2 depend also on the time constant of the corresponding evolutions. γ is the natural rate of recovery under medical control.

Parameters b and c are related to the results of the tests on the suspected cases Q, or to the time of permanence in quarantine; b is the rate of return from the quarantine to the health susceptible people; c denotes the rate of transition from Q to the class corresponding to the results of the test, sane with probability n (negative response), or infected for the remaining $1 - n$, defined according to the average time required for the tests. Since the tests policy can depend from medical or political or economical constraints, the control u_5 is present to allow the quantification of such an intervention. Actually, all the control actions introduced try to include all possible intervention policies in presence of a virus spread for which no vaccine is available. In details, u_1, with an efficacy coefficient a, denotes the action aiming to stimulate, or force, a test campaign on the population with the aim at recognising infected individuals as early as possible to isolate them and, then, reduce the contagious. Control u_2 models the quarantine/isolation indications on health population to keep it far from the possible contagious occasions. It does not correspond to an actual isolation, but to a reduction of the contact occasions simply reducing the interaction with other people. It is bounded between zero and one, where $u_2 = 1$ corresponds to an ideal total individual isolation.

Controls u_3 and u_4 represent the therapy actions: the first one devoted directly to counteract the virus by means of antiviral drugs, and the second one to reduce the side–effects of the induced cardio–respiratory diseases, as long as of possible previous pathologies or different complications. For $u_3(t)$ a coefficient η is introduced to denote the effectiveness of the therapy. As far as $u_4(t)$ is concerned, its effect is introduced as a direct contribution to reduce the mortality rate and it is bounded between zero (no therapy) and 1 (all individuals kept alive during the infection course).

2.2 Stability analysis

The equilibrium points are computed as the solutions of the system

$$B - \beta S^e I_C^e + bnQ^e - d_S S^e = 0 \tag{7}$$

$$\beta S^e I_C^e - kE^e - d_E E^e = 0 \tag{8}$$

$$kE^e - h_1 I_C^e - h_2 I_C^e - d_{I_C} I_C^e = 0 \tag{9}$$

$$h_1 I_C^e + h_1(1-n)Q^e - \gamma I_Q^e - d_{I_Q} I_Q^e = 0 \tag{10}$$

$$-bnQ^e - h_1(1-n)Q^e - d_Q Q^e = 0 \tag{11}$$

$$h_2 I_C^e + \gamma I_Q^e - d_R R^e = 0 \tag{12}$$

One feasible equilibrium point P_1^e is always present for any value of the parameters and corresponds to the so called *disease free* condition. It is given by

$$P_1^e = \begin{pmatrix} S_1^e & E_1^e & I_{C1}^e & I_{Q1}^e & Q_1^e & R_1^e \end{pmatrix}^T = \begin{pmatrix} \frac{B}{d_S} & 0 & 0 & 0 & 0 & 0 \end{pmatrix}^T \tag{13}$$

4

The system can have a second equilibrium point

$$
P_2^e = \begin{pmatrix} S_2^e \\ E_2^e \\ I_{C2}^e \\ I_{Q2}^e \\ Q_2^e \\ R_2^e \end{pmatrix} = \begin{pmatrix} \frac{(k+d_E)(h_1+h_2+d_{I_C})}{\beta k} \\ \frac{(h_1+h_2+d_{I_C})}{k}\left(\frac{kB}{(k+d_E)(h_1+h_2+d_{I_C})}-\frac{d_S}{\beta}\right) \\ \frac{kB}{(k+d_E)(h_1+h_2+d_{I_C})}-\frac{d_S}{\beta} \\ \frac{h_1}{(\gamma+d_{I_Q})}\left(\frac{kB}{(k+d_E)(h_1+h_2+d_{I_C})}-\frac{d_S}{\beta}\right) \\ 0 \\ \left(\frac{h_2(\gamma+d_{I_Q})+\gamma h_1}{d_R(\gamma+d_{I_Q})}\right)\left(\frac{kB}{(k+d_E)(h_1+h_2+d_{I_C})}-\frac{d_S}{\beta}\right) \end{pmatrix} \tag{14}
$$

provided that condition

$$
\frac{kB}{(k+d_E)(h_1+h_2+d_{I_C})}-\frac{d_S}{\beta} \geq 0 \tag{15}
$$

is verified, equivalent to the more compact form

$$
B - d_S S_2^e \geq 0 \tag{16}
$$

The analysis of stability of the computed equilibrium points is an important step to understand the level of dangerousness of the illness.

The local stability characteristics of the equilibrium points can be defined studying the eigenvalues of the Jacobian matrix of the given dynamics evaluated in each of the equilibrium points.

For the dynamics (1)–(6), the expression obtained for the Jacobian, computed for the input equal to zero, is

$$
J = \begin{pmatrix} -\beta I_C - d_S & 0 & -\beta S & 0 & b & 0 \\ \beta I_C & -(k+d_E) & \beta S & 0 & 0 & 0 \\ 0 & k & -(h_1+h_2+d_{I_C}) & 0 & 0 & 0 \\ 0 & 0 & h_1 & -(\gamma+d_{I_Q}) & h_1(1-n) & 0 \\ 0 & 0 & 0 & 0 & -(bn+h_1(1-n)+d_Q) & 0 \\ 0 & 0 & h_2 & \gamma & 0 & -d_R \end{pmatrix} \tag{17}
$$

Thanks to the matrix structure, it is possible to see that three eigenvalues, common for any equilibrium point since independent of the state value, are $\lambda_1 = -d_R$, $\lambda_2 = -(bn+h_1(1-n)+d_Q)$ and $\lambda_3 = -(\gamma+d_{I_Q})$, all real negative for any parameters value. For the remaining three eigenvalues, the reduced matrix

$$
\tilde{J} = \begin{pmatrix} -\beta I_C - d_S & 0 & -\beta S \\ \beta I_C & -(k+d_E) & \beta S \\ 0 & k & -(h_1+h_2+d_{I_C}) \end{pmatrix} \tag{18}
$$

has to be studied. Evaluating (18) in the equilibrium point P_1^e (13), it becomes

$$
\tilde{J}(P_1^e) = \begin{pmatrix} -d_S & 0 & -\frac{\beta B}{d_S} \\ 0 & -(k+d_E) & \frac{\beta B}{d_S} \\ 0 & k & -(h_1+h_2+d_{I_C}) \end{pmatrix} \tag{19}
$$

5

for which $\lambda_4 = -d_S$ is directly obtained while for the last two eigenvalues the roots of the equation

$$\lambda^2 + (k + h_1 + h_2 + d_E + d_{I_C})\lambda + \left((k + d_E)(h_1 + h_2 + d_{I_C}) - \frac{\beta k B}{d_S}\right) = 0 \quad (20)$$

must be computed. By Descartes' rule of signs, the two solutions λ_5 and λ_6 of (20) have negative real part if and only if

$$(k + d_E)(h_1 + h_2 + d_{I_C}) - \frac{\beta k B}{d_S} > 0 \quad (21)$$

Since, from (15) and (16),

$$(k + d_E)(h_1 + h_2 + d_{I_C}) - \frac{\beta k B}{d_S} = -\beta(B - d_S S_1^e) \quad (22)$$

it is possible to conclude that P_1^e is locally asymptotically stable, P_2^e is not feasible, that is the system has only the *epidemic free* equilibrium point locally asymptotically stable.

If (21) is not satisfied, and then (15) is, the second equilibrium point P_2^e as in (14) exists, while the equilibrium point P_1^e becomes unstable. The stability of P_2^e can be studied evaluating the reduced Jacobian matrix (18) in such a point. The result is

$$\tilde{J}(P_2^e) = \begin{pmatrix} -\beta I_{C2}^e - d_S & 0 & -\beta S_2^e \\ \beta I_{C2}^e & -(k + d_E) & \beta S_2^e \\ 0 & k & -(h_1 + h_2 + d_{I_C}) \end{pmatrix} \quad (23)$$

and its characteristic polynomial is

$$\lambda^3 + C_2\lambda^2 + C_1\lambda + C_0 \quad (24)$$

with

$$C_2 = \frac{B}{S_2^e} + k + d_E + h_1 + h_2 + d_{I_C} \quad (25)$$

$$C_1 = \frac{B}{S_2^e}(k + d_E + h_1 + h_2 + d_{I_C}) \quad (26)$$

$$C_0 = B\beta k - d_S(k + d_E)(h_1 + h_2 + d_{I_C}) = \beta k (B - d_S S_2^e) \quad (27)$$

where

$$\beta I_{C2}^e + d_S = \frac{B}{S_2^e} \quad (28)$$

has been used.

Making use of the Routh–Hurwitz criterion, the roots of (24) have negative real part if and only if

$$C_2 > 0, \quad C_1 C_2 - C_0 > 0, \quad C_0 > 0 \quad (29)$$

Condition $C_2 > 0$ always holds. Also the second one is verified for any choice of parameters values, since, after some computations, one has

$$
\begin{aligned}
C_1 C_2 - C_0 &= \beta k \left(B + d_S S_2^e \right) + \left(\frac{B}{S_2^e} \right)^2 \left(k + d_E + h_1 + h_2 + d_{I_C} \right) \\
&\quad + \frac{B}{S_2^e} \left((k + d_E)^2 + (h_1 + h_2 + d_{I_C})^2 \right)
\end{aligned}
\tag{30}
$$

always positive. As long as the third condition, one has

$$
B - d_S S_2^e > 0
\tag{31}
$$

This result shows that the local stability condition for the equilibrium point P_2^e coincides with its existence one. Then, it is possible to summarise such results saying that if the values of the parameters do not satisfy condition (15), the system admits only one equilibrium point, P_1^e, locally asymptotically stable; on the other hand, under the fulfilment of (15), also a second feasible equilibrium point exists, P_2^e, locally asymptotically stable, while the first one, P_1^e, becomes unstable. In this case, the presence of a bifurcation characterises the stability of the system equilibria, as usually happens in epidemic spreads models [7].

2.3 The basic reproduction number

An important parameter which usually characterises an epidemic spread is the basic reproduction number R_0 [31]: it gives a numerical valuation of the infectivity of the virus: a value higher than 1 characterises expansive infections, while for a value smaller than 1, the spread autonomously decreases.

There are different approaches for the evaluation or the estimation of R_0 for an epidemic spread. Starting from the mathematical model of the epidemic spread, a relationship between R_0 and the model parameters can be obtained using the next generation matrix approach. The computation starts from the consideration of the part of the dynamics (1)–(6) which describes the classes directly involved in the spread of the infection, in our case E and I_C,

$$
\begin{aligned}
\dot{E}(t) &= \beta S(t) I_C(t) - k E(t) - d_E E(t) \tag{32} \\
\dot{I}_C(t) &= k E(t) - h_1 I_C(t) - h_2 I_C(t) - d_{I_C} I_C(t) \tag{33}
\end{aligned}
$$

and, after reordering the expressions separating the contagious terms from the transition as

$$
\begin{pmatrix} \dot{E}(t) \\ \dot{I}_C(t) \end{pmatrix} = \begin{pmatrix} \beta S(t) I_C(t) \\ 0 \end{pmatrix} - \begin{pmatrix} (k + d_E) E(t) \\ (h_1 + h_2 + d_{I_C}) I_C(t) - k E(t) \end{pmatrix} = \mathcal{F} - \mathcal{V} \tag{34}
$$

the two matrices

$$
F = \left. \frac{\partial \mathcal{F}}{\partial (E, I_C)} \right|_{P_1^e} = \begin{pmatrix} 0 & \beta \frac{B}{d_S} \\ 0 & 0 \end{pmatrix}
\tag{35}
$$

and

$$V = \frac{\partial \mathcal{V}}{\partial(E, I_C)}\bigg|_{P_1^e} = \begin{pmatrix} k + d_E & 0 \\ -k & h_1 + h_2 + d_{I_C} \end{pmatrix} \tag{36}$$

are computed. Under these positions, R_0 is given by the dominant eigenvalue of the matrix FV^{-1}

$$FV^{-1} = \begin{pmatrix} \beta \frac{B}{d_S} \frac{k}{(k+d_E)(h_1+h_2+d_{I_C})} & \beta \frac{B}{d_S} \frac{1}{h_1+h_2+d_{I_C}} \\ 0 & 0 \end{pmatrix} \tag{37}$$

from which

$$R_0 = \frac{\beta k B}{d_S(k + d_E)(h_1 + h_2 + d_{I_C})} \tag{38}$$

If (38) is rewritten as

$$R_0 = \frac{B}{d_S S_2^e} = \frac{B - d_S S_2^e}{d_S S_2^e} + 1 \tag{39}$$

it is easy to observe that condition $R_0 > 1$ is equivalent to $B - d_S S_2^e > 0$. This confirms that when $R_0 < 1$ and the epidemic does not spread, the dynamics has only the *epidemic free* equilibrium condition, asymptotically stable. On the other hand, when $R_0 > 1$ and the epidemic spreads, the asymptotically stable equilibrium point is the *endemic* one, P_2^e, which is, in this case, admissible.

Such values are homogeneous with the equivalent ones present in literature [15], [16]. The correspondence supports the correctness of the present physically driven choice of the values.

In next Section 3 numerical evaluations of the effects of the different possible lines of intervention, represented by the four controls $u_i(t)$, $i = 1, 2, 3, 4, 5$, are reported and discussed.

3   Evaluation of the effectiveness of intervention actions

In this Section the effects on the epidemic evolution of the five different control actions are numerically illustrated and analysed.

For each control, a set of different values has been chosen and the consequent time histories of the state variables are reported and discussed.

The values fixed for the parameters are in Table 1. A discussion on the considerations followed for obtaining such values is contained in [32]. The case of the Wuhan region has been considered for the definition of statistical data used.

All the simulations have been performed starting from initial conditions $S(0) = 59.17 \cdot 10^6$, the population of the considered Region at the beginning of the epidemic, $E(0) = 4$, $I_C(0) = 2$, $I_Q(0) = 1$, so that the results start with the discovery of the first positive patients, $Q(0) = 0$ and $R(0) = 0$.

8

Table 1: Numerical values of the model parameters: comparative table for equivalent terms

Parameter	B	β	k	h_1	h_2	γ
Value	1180	$2.5 \cdot 10^{-8}$	$1/7$	$\phi/3$	$(1-\phi)/15$	$1/15$
Parameter	a	b	c	η	n	ϕ
Value	a	$n/15$	$1/2$	η	0.95	0.9
Parameter	d_S	d_E	d_{I_C}	d_{I_Q}	d_Q	d_R
Value	$2 \cdot 10^{-5}$	$2 \cdot 10^{-5}$	$2 \cdot 10^{-5}$	0.0057	$2 \cdot 10^{-5}$	$2 \cdot 10^{-5}$

3.1 Effects of preventive quarantine $u_1(t)$
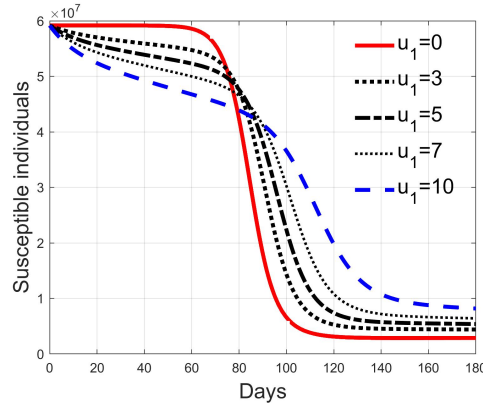
Figure 1: Susceptible individuals for different amplitude of control $u_1(t)$ when 5% of quarantined is infected

The effects of the control action given by $u_1(t)$ is here presented and discussed.

This input corresponds to the choice of quarantining a fraction of the population or because suspected to be infected or for a test campaign. Since the test campaign corresponds to the action modelled by the input $u_5(t)$, if only input $u_1(t)$ is active, only the isolation of suspected individuals is now considered, kept in quarantine for a safe period (15 days), or until the symptoms appear.

In this short analysis, to better put in evidence if and when this action can be fruitful, two cases are considered: one in which the number of possible infected people among the quarantined is low, set equal to the 5% of them, and one on which the fraction of infected is higher, fixed to the 20%.

Simulations have been performed varying $u_1(t)$ between zero (no action) and 10; in the Figures 1 and 2 the time history of the susceptible individuals
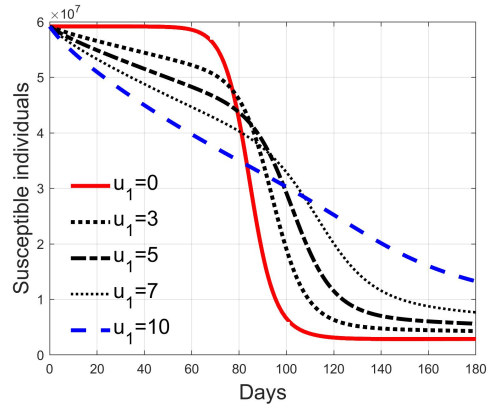
Figure 2: Susceptible individuals for different amplitude of control $u_1(t)$ when 20% of quarantined is infected
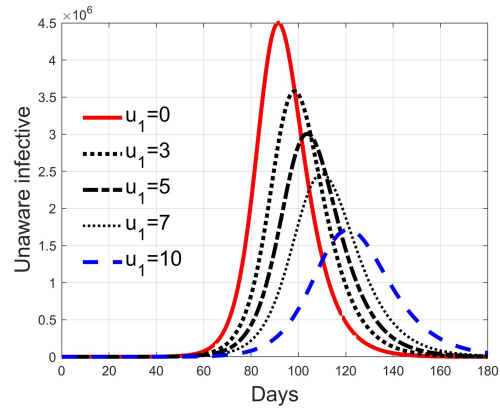
Figure 3: Infected asymptomatic individuals for different amplitude of control $u_1(t)$ when 5% of quarantined is infected
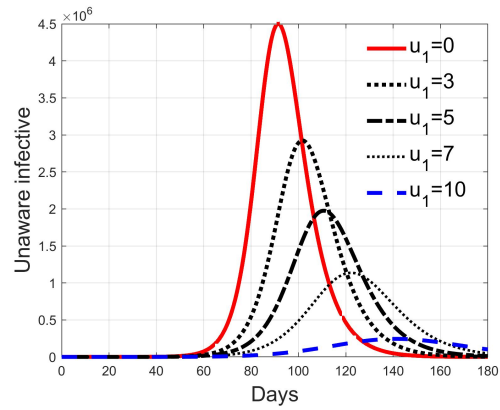
Figure 4: Infected asymptomatic individuals for different amplitude of control $u_1(t)$ when 20% of quarantined is infected
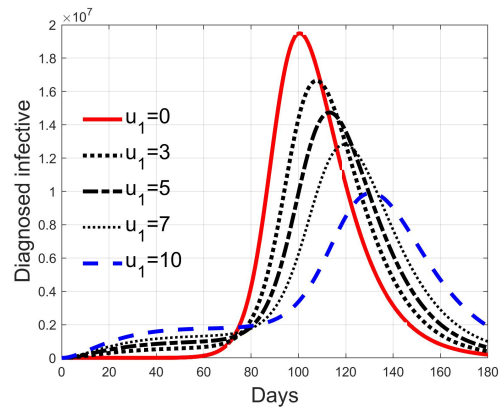

Figure 5: Infected diagnosed individuals for different amplitude of control $u_1(t)$ when 5% of quarantined is infected

11
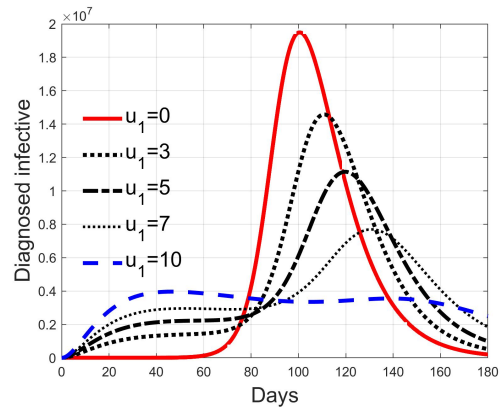
Figure 6: Infected diagnosed individuals for different amplitude of control $u_1(t)$ when 20% of quarantined is infected
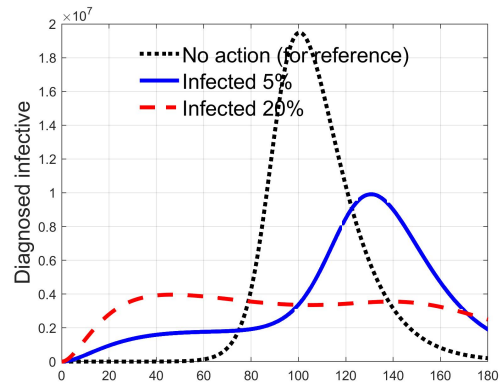
Figure 7: Comparison between infected diagnosed individuals for the 5% and 20% cases of quarantined infected, when $u_1 = 10$
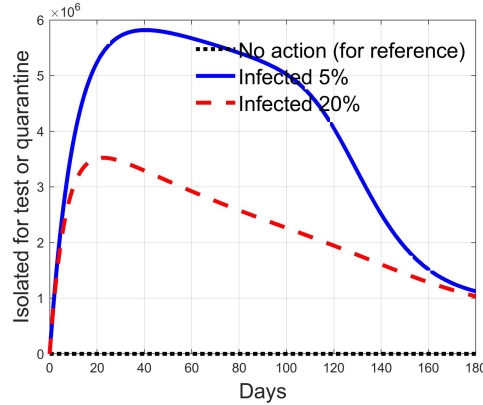
Figure 8: Comparison between quarantined individuals for the 5% and 20% cases among them, when $u_1 = 10$

is reported for the case of 5% and 20% of infected respectively. Clearly, the higher is the control amplitude, the higher is the initial decrement of the class due to the fact that a larger part is put in quarantine. However, this behaviour holds until the number of the infected individuals which can infect, the ones before the symptoms or totally asymptomatic, increases, as can be observed from Figures 3 and 4. After the peak of infective persons, a higher control input produces a lower rate of decrement in the susceptible class. The important result arises from Figures 5 and 6 where the diagnosed infected individuals are reported for the two considered percentages. In fact, a delay of the peak as well as the reduction of its amplitude can be appreciated, more sensible for higher probability of infected individuals in the quarantined group, Figure 6. This aspect is well evidenced in Figure 7 where the case $u_1(t) = 10$ is reported for the two cases of 5% and 20% of infected among the quarantined persons, along with the case of no action for reference purpose. It can be even observed a sort of flattening in the time evolution of the diagnosed infected patients exceptional for high rate of quarantine and high probability to have an infected individual in the quarantined group. With this action, the number of individuals put in quarantine, depicted in Figure 8 for the same cases as in Figure 7, presents a significant level, more acceptable when the infection probability is higher. In fact, for the two cases here addressed, when the percentage of infected is 5%, the value of more than the 8% of the initial population (about 5 millions) for more than 90 days is reached, while when 20% is considered, the maximum value assumed is 3.5 millions and decreases at a rate of more than 16600 a day.

13
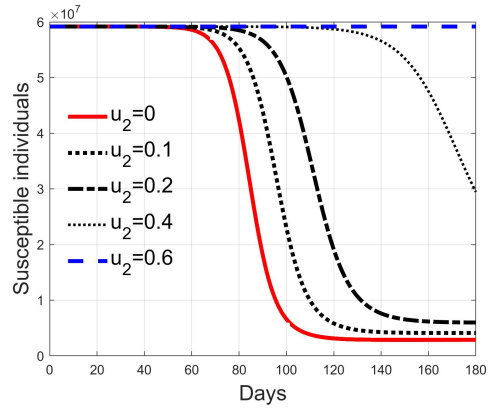
Figure 9: Susceptible individuals for different values of $u_2(t)$
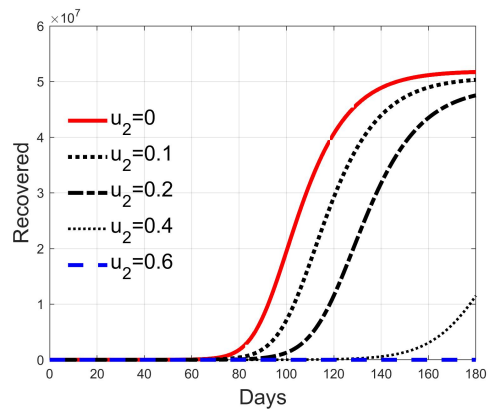
Figure 10: Recovered individuals for different values of $u_2(t)$

14
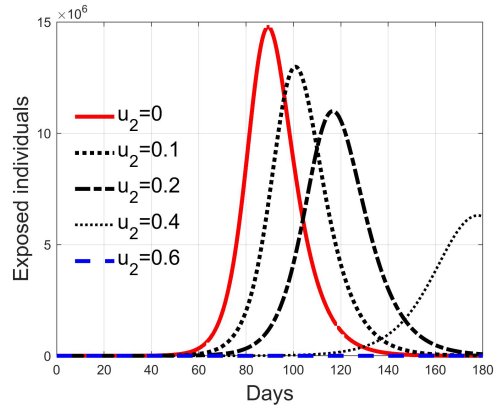
Figure 11: Exposed individuals for different values of $u_2(t)$
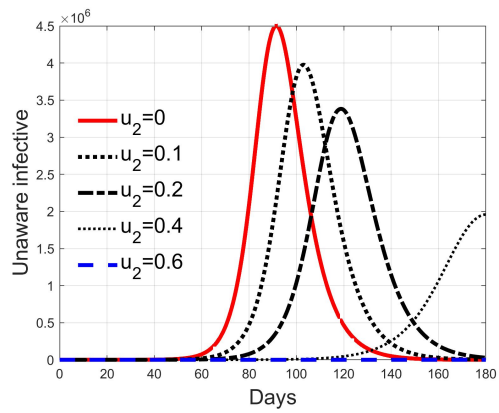
Figure 12: Infected asymptomatic individuals for different values of $u_2(t)$

15
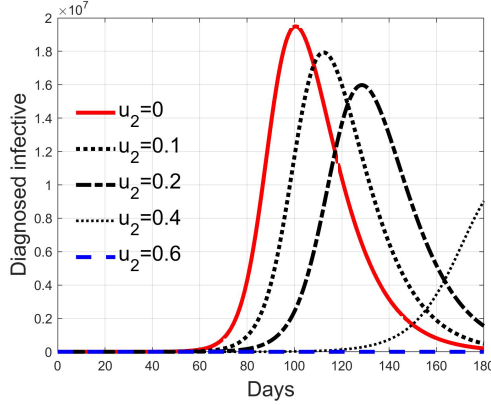
Figure 13: Infected diagnosed individuals for different values of $u_2(t)$

3.2 Effects of isolation $u_2(t)$

This control represents an action which aims at reducing the contact rate between susceptible and infected individuals. This can be obtained by means of a generalised quasi-isolation of the population, for example suggesting or imposing to people to stay at their own home as much time as possible, closing some activities like schools, offices, factories, shops and so on, so decreasing the possibilities of contacts.

Its effect reduces the nominal contact rate β. Thanks to the relationship between β and R_0, it is possible to compute the minimum value for $u_2(t)$ to obtain a basic reproduction number smaller than 1 once the epidemic characteristics of the transmission, given by β is fixed. In fact, it is possible to write

$$\tilde{R}_0 = \frac{\beta(1 - u_2)kB}{d_S(k + d_E)(h_1 + h_2 + d_{I_C})} = R_0(1 - u_2) \tag{40}$$

where R_0 is the initial reproduction number and $\tilde{R}_0 < R_0$ is the one resulting under the action of the control. Then

$$u_2 = 1 - \frac{\tilde{R}_0}{R_0} \tag{41}$$

and the lowest value $u_{2,min}$ to have $\tilde{R}_0 \leq 1$ is given by

$$u_{2,min} = 1 - \frac{1}{R_0} = 0.6875 \tag{42}$$

In Figures 9–13 the results of simulation for different values of $u_2(t) \in [0, 0.6]$ are reported. The five cases considered correspond, for what said above, to cases of epidemic with $\tilde{R}_0 = R_0 = 3.2$ ($u_2 = 0$), $\tilde{R}_0 = 0.9R_0 = 2.88$ ($u_2 = 0.1$), $\tilde{R}_0 =$

16

$0.8R_0 = 2.56$ ($u_2 = 0.2$), $\tilde{R}_0 = 0.6R_0 = 1.92$ ($u_2 = 0.4$) and $\tilde{R}_0 = 0.4R_0 = 1.28$ ($u_2 = 0.6$). In fact, the curves in each figure have the same shape as epidemic spreads with different reproduction number. Then, it can be concluded that increasing $u_2(t)$, the spread is reduced and delayed in time, making the epidemic more controllable. For values sufficiently high, greater than $u_{2,min}$, the epidemic dynamics changes its characteristics and the disease free equilibrium becomes stable. It is interesting to note the correspondence of expression (42) with the condition for herd immunity.

3.3   Effects of antiviral therapy $u_3(t)$
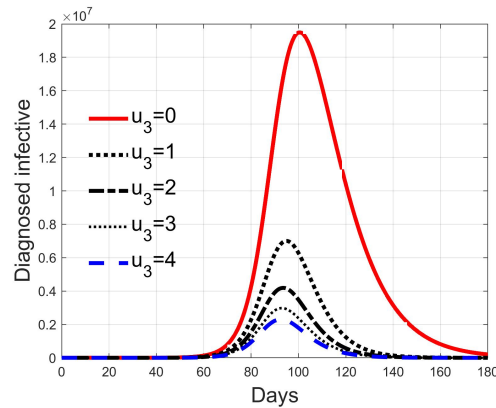
Figure 14: Infected diagnosed individuals for different values of control $u_3(t)$

This control acts on the diagnosed infected patients to reduce and contrast the virus effects so facilitating and reducing the time for healing. Figure 14 depicts the time history of the number of such patients for the cases of $u_3(t) = 0, 1, 2, 3, 4$. Thanks to the direct effect of such a control, the peak values are strongly reduced and this effect reflects on the number of deaths, as can be noted in Figure 15 where the ratio between the deaths of infected patients and the standard deaths is plotted. This result shows that, if available, an antiviral therapy produces highly positive effects for the infection contrast.

3.4   Effects of therapy against complications $u_4(t)$

Like the previous one, this control produces effects on the diagnosed infected patients but, differently from $u_3(t)$, $u_4(t)$ represents the efficacy of the therapy for the effects induced by the virus and for the possible complications. Its goal is to keep alive the patient during the natural development and evolutions of the individual anti–viruses, for example with intensive care and respiratory supports. The consequence is that it reduces the death rate, as depicted in
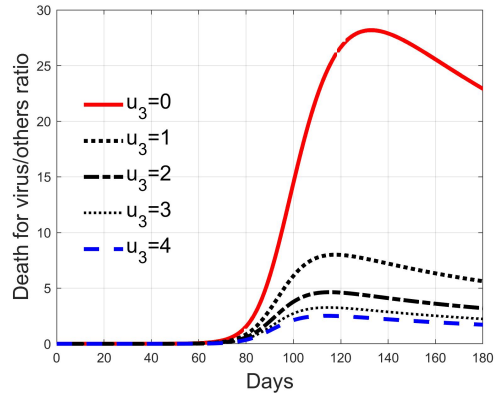
Figure 15: Ratio between deaths by virus and other deaths, for different values of control $u_3(t)$
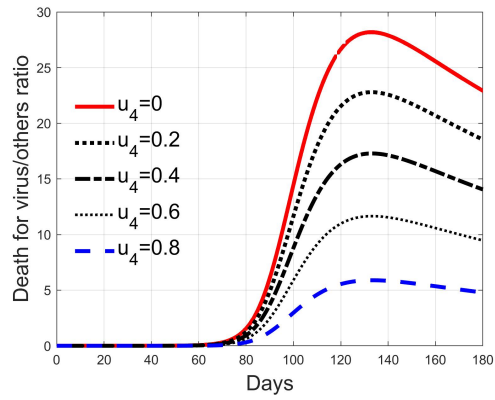

Figure 16: Ratio between deaths by virus and other deaths, for different values of control $u_4(t)$
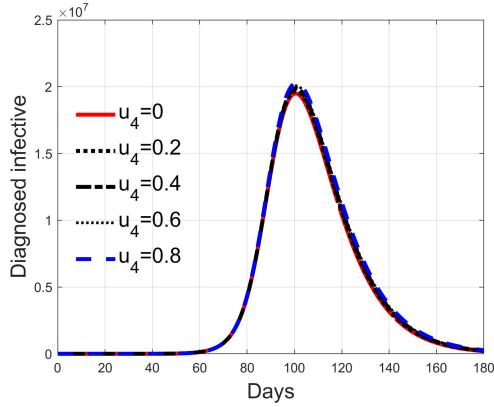
Figure 17: Infected diagnosed individuals for different values of control $u_4(t)$

Figure 16, but not affect sensibly the number of isolated and treated individuals, in Figure 17 since, differently from the case of input $u_3(t)$, this action does not remove more quickly patients from the class but keep them there for all the illness period. In Figure 16 it is clear the reduction of the deaths, 28 times the normal quantities at the peak with $u_4(t) = 0$, which becomes 6 times with $u_4(t) = 0.8$, decreasing almost linearly.

3.5 Effects of amount of tests $u_5(t)$
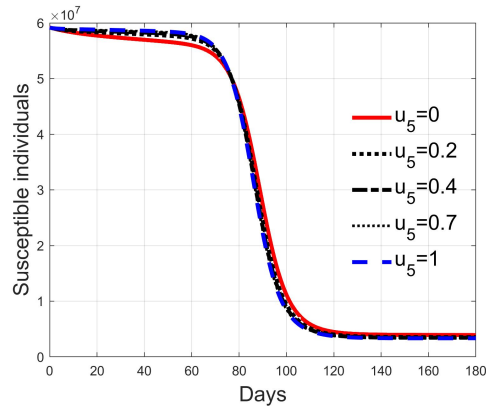
Figure 18: Susceptible individuals S for low rate of quarantine transfer ($u_1(t) = 2$) and low percentage of infected among them (5%)
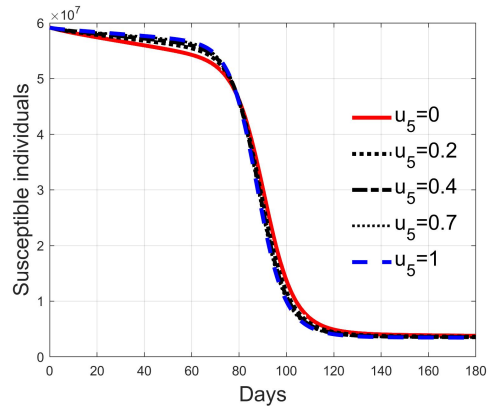
Figure 19: Susceptible individuals S for low rate of quarantine transfer ($u_1(t) = 2$) and high percentage of infected among them (20%)
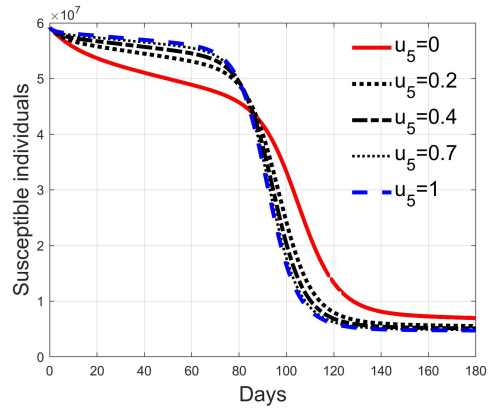

Figure 20: Susceptible individuals S for high rate of quarantine transfer ($u_1(t) = 8$) and low percentage of infected among them (5%)
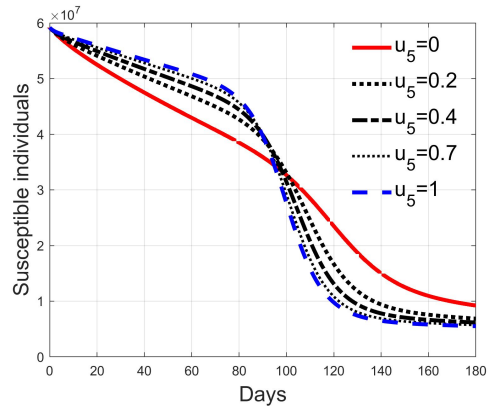
Figure 21: Susceptible individuals S for high rate of quarantine transfer ($u_1(t) = 8$) and high percentage of infected among them (20%)
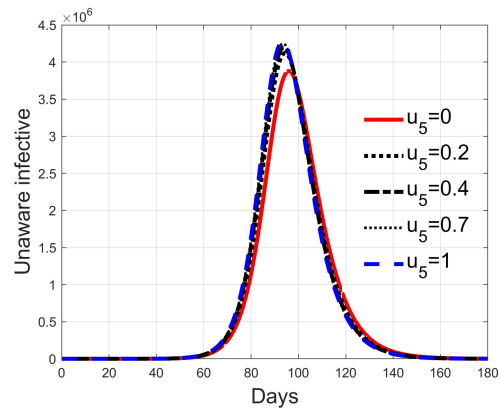

Figure 22: Infective individuals I_C for low rate of quarantine transfer ($u_1(t) = 2$) and low percentage of infected among them (5%)

21
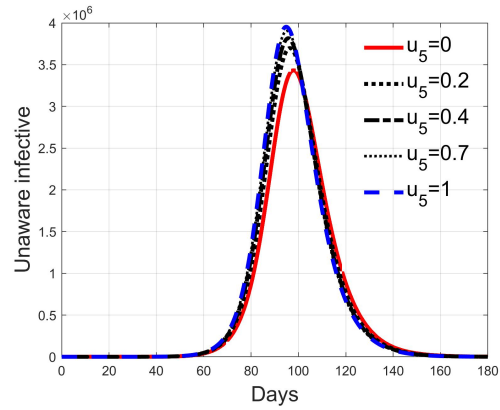
Figure 23: Infective individuals I_C for low rate of quarantine transfer $(u_1(t) = 2)$ and high percentage of infected among them (20%)
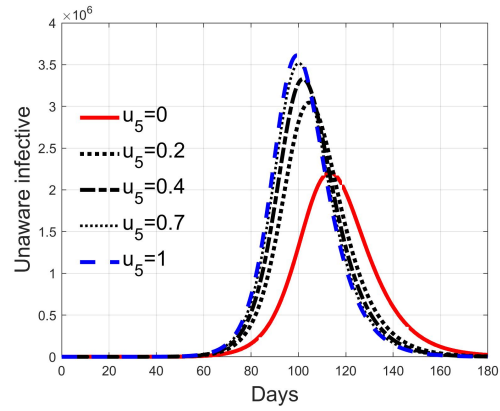

Figure 24: Infective individuals I_C for high rate of quarantine transfer $(u_1(t) = 8)$ and low percentage of infected among them (5%)
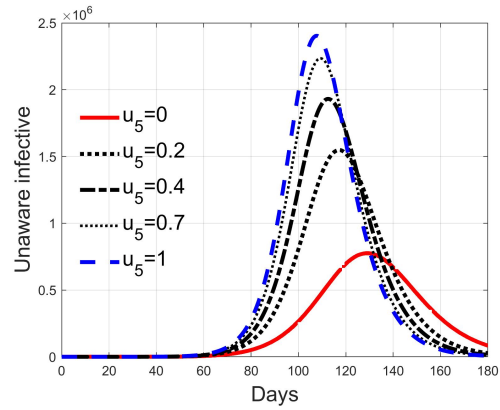
Figure 25: Infective individuals I_C for high rate of quarantine transfer ($u_1(t) = 8$) and high percentage of infected among them (20%)
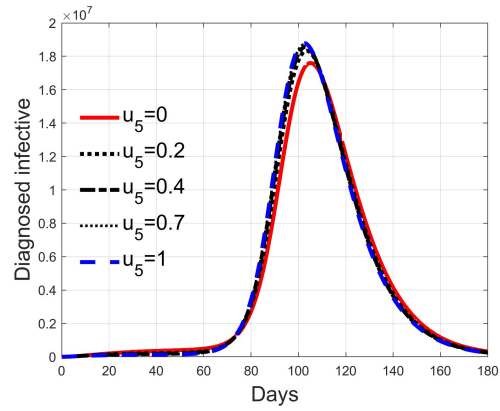

Figure 26: Infected diagnosed individuals I_Q for low rate of quarantine transfer ($u_1(t) = 2$) and low percentage of infected among them (5%)
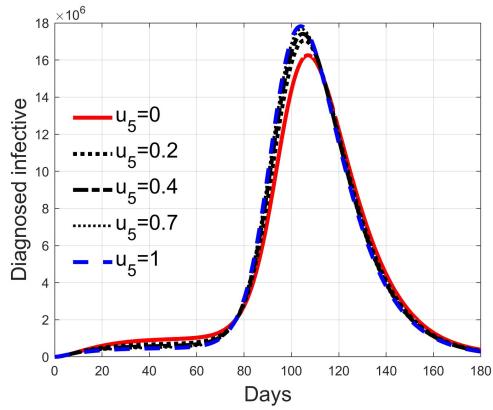
Figure 27: Infected diagnosed individuals I_Q for low rate of quarantine transfer $(u_1(t) = 2)$ and high percentage of infected among them (20%)
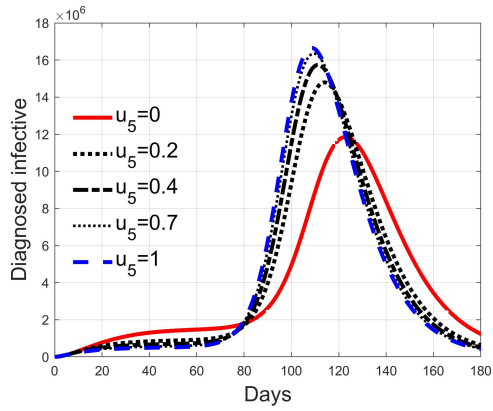
Figure 28: Infected diagnosed individuals I_Q for high rate of quarantine transfer $(u_1(t) = 8)$ and low percentage of infected among them (5%)

24
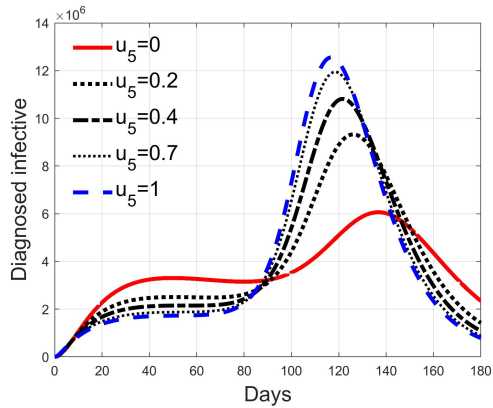
Figure 29: Infected diagnosed individuals I_Q for high rate of quarantine transfer $(u_1(t) = 8)$ and high percentage of infected among them (20%)
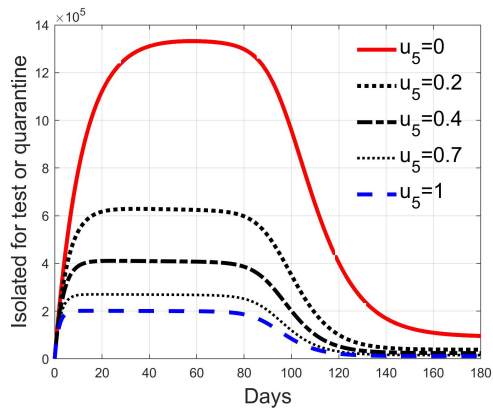
Figure 30: Quarantined individuals Q for low rate of quarantine transfer $(u_1(t) = 2)$ and low percentage of infected among them (5%)

25
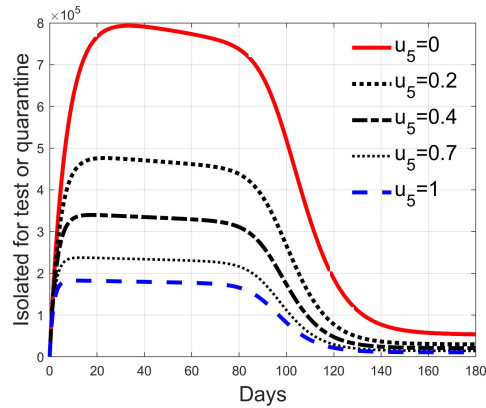
Figure 31: Quarantined individuals Q for low rate of quarantine transfer $(u_1(t) = 2)$ and high percentage of infected among them (20%)
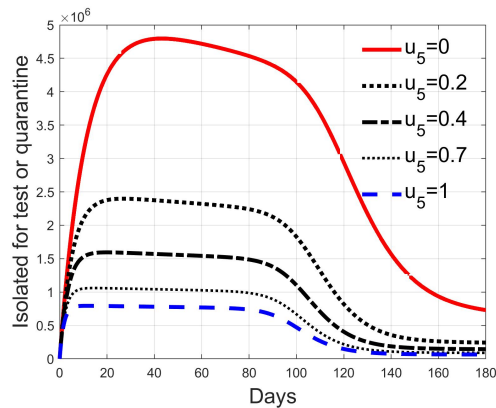

Figure 32: Quarantined individuals Q for high rate of quarantine transfer $(u_1(t) = 8)$ and low percentage of infected among them (5%)

26
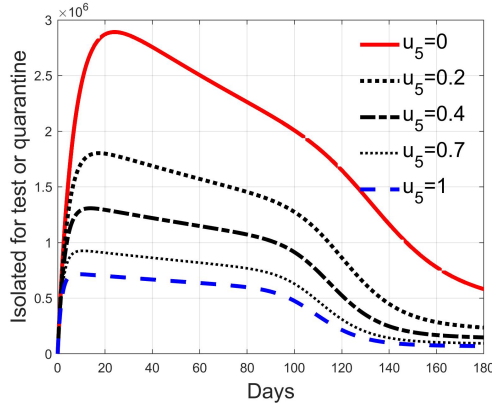
Figure 33: Quarantined individuals Q for high rate of quarantine transfer $(u_1(t) = 8)$ and high percentage of infected among them (20%)

The control input $u_5(t)$ represents the amount of test performed on the population. In this model, the people to be tested are temporarily considered as quarantined. Moving people to quarantine status can be done by means of input u_1 only. Then, in order to analyse the effect of different levels of test rate, the input $u_1(t)$ must be set to a value different to zero. Moreover, as remarked in subsection 3.1, the effect of putting in quarantine persons is dependent on the hypothesised number of positive results.

These considerations motivate the choice of four cases, obtained combining the cases of high and low value for $u_1(t)$, chosen equal to 2 and 8 respectively, with the cases of high and low percentage of expected positive tests, the two already considered values of 20% and 5%. For each of these four cases, the input $u_5(t)$ is varied in the interval $[0, 1]$.

In Figures 18–21 the effects on the susceptible class are presented. Figures 18 and 19 both refer to the case of low rate of motion to the quarantine status $(u_1(t) = 2, 0.2\%$ of susceptible people a day), the first one for a low fraction of infected (5%, $n = 0.95$) and the second one for a high number (20%, $n = 0.8$). Figures 20 and 21 have the same meaning but with a higher rate of transfer to quarantine for test $(u_1(t) = 8)$.

Figures 26–29 depict the diagnosed infected while Figures 30–33 refers to the quarantined individuals, always with the same order for $u_1(t)$ and n as for the susceptible individuals.

Recalling that the case of $u_5(t) = 0$ refers to a pure quarantine policy, analysed in Subsection 3.1, the most evident result is that, testing the quarantined persons and letting the negative ones return to the susceptible class has the consequence to increase the epidemic spread from the outbreak of the virus until the peak of the infection, anticipated in time and increased in amplitude. In fact, in this time interval, the number of susceptible persons decreases slower

27

as $u_5(t)$ increases, as observable in Figures 18–21, since a high number of tests let many negative individuals return in such a class instead of remaining in the quarantine one longer. Even if some exposed and asymptomatic are found and isolated, the decrement of the infective individuals is compensated by the increment of the susceptible persons, in Figures 22–25, with the consequence of having more infected patients. During this time, the number of diagnosed individuals is lower, Figures 26–29, probably because the total time of transition from the susceptible to the diagnosed class for all the not tested individuals is longer than from quarantine to diagnosis.

In correspondence of the peak of infected, the number of susceptible persons presents a fast decrement, as usual in epidemics spread, but in this case the velocity of the decrement is directly related to the number of tests. From the point of view of the diagnosed infective patients, after the initial period with a slow increment, the evolution follows the same behaviour as all the infected classes, with its peak and the subsequent decrement.

The quarantined class is highly affected by the different choices, as Figures 30–33 show. In fact, it can be appreciated how much the number of tests contributes to the class empting.

This phenomenon is related to the initial behaviour of the diagnosed individuals discussed above: empting the quarantine class corresponds to reduce the isolation and to have, along the illness course, the asymptomatic infective class more filled, with consequences on the velocity of the spread.

4   Conclusions

In this paper a new mathematical model for describing the spread of a virus in absence of vaccination is used for the analysis of the effects of the considered controls, showing their effects on the different classes of population modelled. The model is designed to include all the possible active actions, both from the political point of view and the medical one. A first set of inputs are devoted to the containment of the spread thorough induced social behaviours, a second one concerns the possible therapies that can be applied. The parameters ar fixed to fit the behaviour of the COVID-19 in the Wuhan region at the beginning of the infection detection. After a discussion on the influence of some parameters on the dynamical behaviour of the virus spread, an

This analysis is a first step to help to a better forecast of the effects of possible choices to be adopted. For example, it can help to dimension the quarantined class and the tests to have an acceptable number of isolated individuals without increasing too much the number of the infected ones, or to define the maximum levels of available medical cares to dimension the isolation and the quarantine actions, and so on.

References

[1] W. O. Kermack and A. G. McKendrick, "A contribution to the mathematical theory of epidemics," *Proc. Roy. Soc. Lond. A*, vol. 115, no. 772, pp. 700–721, 1927.

[2] R. Casagrandi, L. Bolzoni, S. Levin, and V. Andreasen, "The SIRC model and influenza," *A. Mathematical Biosciences*, vol. 200, 2006.

[3] R. Naresh, A. Tripathi, and D. Sharma, "Modeling and analysis of the spread of AIDS epidemic with immigration of HIV infectives," *Mathematical and Computer Modelling*, vol. 49, 2009.

[4] T. Vasanthi and V. Vijayalakshmi, "Mathematical models for the study of HIV/AIDS epidemics," *proc. IEEE International Conference on advances in Engineering, Science and Management*, pp. 108–112, 2012.

[5] U. S. Basak, B. K. Datta, and P. K. Ghose, "Mathematical analysis of an HIV/AIDS epidemic model," *Amer.J.Math Stat*, vol. 5, no. 5, pp. 253–258, 2015.

[6] P. Di Giamberardino and D.Iacoviello, "Optimal control to reduce the HIV/AIDS spread," *22nd International Conference on System Theory, Control and Computing*, 2018.

[7] P. Di Giamberardino, L. Compagnucci, C. D. Giorgi, and D. Iacoviello, "Modeling the effects of prevention and early diagnosis on HIV/AIDS infection diffusion," *IEEE Transactions on Systems, Man and Cybernetics: Systems*, 2019.

[8] P. Di Giamberardino and D. Iacoviello, "Epidemic modeling and control of HIV/AIDS dynamics in populations under external interactions: a worldwide challenge," *Control Applications for Biomedical Engineering Systems, Elsevier*, 2020.

[9] R. T. Perry and N. A. Halset, "The clinical significance of measles: a review," *The Journal of Infectious Diseases*, vol. 189, no. 1, pp. 4–16, 2004.

[10] O. O. Onyejekwe and E. Z. Kebede, "Epidemiological modeling of measles infection with optimal control of vaccination and supportive treatment," *Applied and computational mathematics*, vol. 4, no. 4, pp. 264–274, 2015.

[11] S. O. Adewale, I. A. Olopade, S. O. Ajao, and G. A. Adeniran, "Optimal control analysis of the dynamical spread of measles," *International Journal of research*, vol. 4, no. 5, pp. 169–188, 2016.

[12] P. Di Giamberardino and D. Iacoviello, "Analysis, simulation and control of a new measles epidemic model," *ICINCO 2019 - Proceedings of the 16th International Conference on Informatics in Control, Automation and Robotics*, 2019.

[13] ——, "Modeling and control of an epidemic disease under possible complication," *Proceedings of the 22nd International Conference on System Theory, Control and Computing*, pp. 67–72, 2018.

[14] C.-C. Lai, T.-P. Shih, W.-C. Ko, H.-J. Tang, and P.-R. Hsueh, "Severe acute respiratory syndrome coronavirus 2 (SARS-CoV-2) and coronavirus disease-2019 (COVID-19): The epidemic and the challenges," *International Journal of Antimicrobial Agents*, In press.

[15] B. Tang, X. Wang, Q. Li, N. L. Bragazzi, S. Tang, Y. Xiao, and J. Wu, "Estimation of the transmission risk of the 2019-nCoV and its implication for public health interventions," *Journal of Clinical Medicine*, vol. 9, no. 2, 2020.

[16] B. Tang, N. L. Bragazzi, Q. Li, S. Tang, Y. Xiao, and J. Wu, "An updated estimation of the risk of transmission of the novel coronavirus (2019-nCov)," *Infectious Disease Modelling*, vol. 5, pp. 248–255, 2020.

[17] J. T. Wu, K. Leung, and G. M. Leung, "Nowcasting and forecasting the potential domestic and international spread of the 2019-nCoV outbreak originating in Wuhan, China: a modelling study," *The Lancet*, 2020.

[18] S. Zhao, Q. Lin, J. R. S. S. Musa, G. Yang, W. Wang, Y. Lou, D. Gao, L. Yang, D. He, and M. H. Wang, "Preliminary estimation of the basic reproduction number of novel coronavirus (2019-nCoV) in China, from 2019 to 2020: A data-driven analysis in the early phase of the outbreak," *International Journal of Infectious Diseases*, vol. 92, pp. 214–217, 2020.

[19] S. Zhanga, M. Diaob, W. Yuc, L. Peic, Z. Lind, and D. Chena, "Estimation of the reproductive number of Novel Coronavirus (COVID-19) and the probable outbreak size on the Diamond Princess cruise ship: A data-driven analysis," *International Journal of Infectious Diseases*, 2020.

[20] K. Roosa, Y. Lee, R. Luo, A. Kirpich, R. Rothenberg, J. Hyman, P. Yan, and G. Chowell, "Real-time forecasts of the COVID-19 epidemic in China from February 5th to February 24th, 2020," *Infectious Disease Modelling*, vol. 5, pp. 256–263, 2020.

[21] G. Chowell, D. Hincapie-Palacio, J. Ospina, B. Pell, A. Tariq, S. Dahal, S. Moghadas, A. Smirnova, L. Simonsen, and C. Viboud, "Using Phenomenological Models to Characterize Transmissibility and Forecast Patterns and Final Burden of Zika Epidemics," *PLoS Curr.*, vol. 8, 2016.

[22] B. Pell, Y. Kuang, C. Viboud, and G. Chowell, "Using phenomenological models for forecasting the 2015 Ebola challenge," *Epidemics*, vol. 22, pp. 62–70, 2018.

[23] R. Bürger, G. Chowell, and L. Y. Lara-Díaz, "Comparative analysis of phenomenological growth models applied to epidemic outbreaks," *Mathematical Biosciences and Engineering*, vol. 16, no. mbe-16-05-212, pages =.

[24] G. Chowell, A. Tariq, and J. Hyman, "A novel sub-epidemic modeling framework for short-term forecasting epidemic waves," *BMC Med*, vol. 17, 2019.

[25] B. J. Cowling, L. M. Ho, and G. M. Leung, "Effectiveness of control measures during the SARS epidemic in Beijing: a comparison of the R_t curve and the epidemic curve," *Epidemiol. Infect.*, vol. 136, pp. 562–566, 2008.

[26] E. Bakare, A. Nwagwo, and E. Danso-Addo, "Optimal control analyis of an SIR epidemic model with constant recruitment," *International Journal of Applied Mathematical Research*, vol. 3, 2014.

[27] P. Di Giamberardino and D. Iacoviello, "Optimal control of SIR epidemic model with state dependent switching cost index," *Biomedical Signal Processing and Control*, vol. 31, 2017.

[28] ——, "An output feedback control with state estimation for the containment of the HIV/AIDS diffusion," *26th Mediterranean Conference on Control and Automation, MED 2018*, 2018.

[29] ——, "Optimal control to reduce the HIV/AIDS spread," *22nd International Conference on System Theory, Control and Computing (ICSTCC)*, 2018.

[30] D. J. Daley and J. Gani, *Epidemic Modelling: An Introduction*, ser. Cambridge Studies in Mathematical Biology. Cambridge University Press, 1999.

[31] M. Martcheva, "An introduction to mathematical epidemiology," *Text in Applied Mathematics 61, Springer*, 2015.

[32] P. Di Giamberardino and D. Iacoviello, "A control based mathematical model for the evaluation of intervention lines in epidemic spreads without vaccination: the covid-19 case study," *Submitted to IEEE European Journal of Epidemiology Informatics*, 2020.